Cellular/Molecular

Synaptotagmin IV Does Not Alter Excitatory Fast Synaptic Transmission or Fusion Pore Kinetics in Mammalian CNS Neurons

Jonathan T. Ting,[1,2] **Brooke G. Kelley,**[1] **and Jane M. Sullivan**[1,2]

[1]Department of Physiology and Biophysics and [2]Program in Neurobiology and Behavior, University of Washington School of Medicine, Seattle, Washington 98195

Synaptotagmin IV (Syt IV) is a brain-specific isoform of the synaptotagmin family, the levels of which are strongly elevated after seizure activity. The dominant hypothesis of Syt IV function states that Syt IV upregulation is a neuroprotective mechanism for reducing neurotransmitter release. To test this hypothesis in mammalian CNS synapses, Syt IV was overexpressed in cultured mouse hippocampal neurons, and acute effects on fast excitatory neurotransmission were assessed. We found neurotransmission unaltered with respect to basal release probability, Ca^{2+} dependence of release, short-term plasticity, and fusion pore kinetics. In contrast, expression of a mutant Syt I with diminished Ca^{2+} affinity (R233Q) reduced release probability and altered the Ca^{2+} dependence of release, thus demonstrating the sensitivity of the system to changes in neurotransmission resulting from changes to the Ca^{2+} sensor. Together, these data refute the dominant model that Syt IV functions as an inhibitor of neurotransmitter release in mammalian neurons.

Key words: **fusion pore kinetics; kiss-and-run; short-term plasticity; calcium dependence; synaptic release probability; paired-pulse depression**

Introduction

Synaptotagmins (Syts) comprise a large family of proteins that are thought to regulate Ca^{2+}-dependent membrane trafficking. Syts are widely evolutionarily conserved. For example, there are eight identified isoforms in *Drosophila* and 15 in mammals. The salient structural features of Syts typically include a single transmembrane domain and tandem cytoplasmic C2 domains (C2A and C2B) that bind Ca^{2+}. However, the Syt IV isoform contains a naturally occurring amino acid substitution at a key residue for Ca^{2+} coordination within its C2A domain (S244 in rat Syt IV). This substitution impairs Ca^{2+} binding, and therefore the Syt IV C2A domain is considered nonfunctional for Ca^{2+}-dependent interactions (von Poser et al., 1997).

Although Syt IV expression in the adult brain is typically much lower than that of the primary Ca^{2+} sensors Syt I/II, it can be induced rapidly in hippocampus and piriform cortex after stimuli that produce strong depolarization, such as seizure (Vician et al., 1995; Tocco et al., 1996). Syt IV can also exhibit Ca^{2+}-dependent binding to Syt I, and thus, it was proposed that elevated Syt IV protein could form part of the Ca^{2+} sensor to regulate neurotransmission (Ferguson et al., 1999; Littleton et al., 1999). These findings, in the context of the impaired Ca^{2+} binding ability of Syt IV, led to the hypothesis that Syt IV upregulation after seizure is a protective mechanism to reduce neural activity (von Poser et al., 1997; Ferguson et al., 1999; Littleton et al., 1999).

Consistent with the neuroprotective hypothesis, overexpression of Syt IV at the *Drosophila* neuromuscular junction reduced the peak amplitude of synaptic responses (Littleton et al., 1999) (but see Robinson et al., 2002). Additional support has come from investigations of pheochromocytoma 12 (PC12) cell dense-core vesicle exocytosis, in which Syt IV overexpression inhibits evoked secretion (Wang et al., 2001; Machado et al., 2004), reduces spike frequency and time from fusion pore opening to dilation (Wang et al., 2001), and increases the frequency and duration of "kiss-and-run" versus full fusion events (Wang et al., 2003). As a result of this mounting evidence from Syt IV overexpression studies, the inducible release-inhibitor hypothesis has grown into the dominant model of Syt IV function.

Here, we provide the first report of acute effects of Syt IV upregulation on excitatory fast synaptic transmission in a mammalian CNS synapse preparation. Although the upregulated Syt IV protein is trafficked to Syt I-containing synaptic vesicles, the electrophysiological evidence argues strongly against the dominant model that Syt IV upregulation serves to inhibit neurotransmitter release. We also provide evidence that Syt IV does not alter

Received Sept. 20, 2005; revised Nov. 9, 2005; accepted Nov. 10, 2005.

This work was supported by the Whitehall Foundation, Klingenstein Fund, and University of Washington Royalty Research Fund (J.M.S.); a National Research Service Award Predoctoral Fellowship (1F31NS051906-01) from the National Institute of Neurological Disorders and Stroke (J.T.T.); and a T32 Postdoctoral Fellowship (DA07278-10) from the National Institute on Drug Abuse (B.G.K.). We thank Greg Ferguson for providing the original rat Syt IV cDNA, Sandy Bajjalieh for generous assistance with the coimmunoprecipitation assay, David Perkel and Sandy Bajjalieh for valuable discussions and comments on this manuscript, Ken Custer for providing custom data analysis software, and Mike Ahlquist and Pat Kensel-Hammes for excellent technical assistance.

Correspondence should be addressed to Jane M. Sullivan, Department of Physiology and Biophysics, Box 357290, University of Washington School of Medicine, Seattle, WA 98195-7290. E-mail: jmsull@u.washington.edu.

DOI:10.1523/JNEUROSCI.3997-05.2006

 0270-6474/06/260372-09$15.00/0

fusion pore kinetics or promote a switch to the kiss-and-run mode of exocytosis at mammalian CNS synapses.

Materials and Methods

Cell culture

Microisland cultures for electrophysiology. Microisland cultures of hippocampal neurons were prepared essentially as described previously (Bekkers and Stevens, 1991). In brief, the CA1–CA3 region of postnatal (postnatal day 0–1) mouse hippocampus was dissociated to a single-cell suspension in neuronal medium and then plated at very low density (3000 cells/ml) onto astrocyte-covered microislands of collagen/poly-D-lysine. The neuronal medium consisted of MEM supplemented with 10% horse serum, 20 mM glucose, 0.85% Glutamax, 25 mM HEPES, 1 mM sodium pyruvate, and penicillin/streptomycin.

Conventional cultures for biochemistry. High-density (200,000–400,000 cells/ml) cultures of hippocampal neurons were prepared for coimmunoprecipitation assays. Culture conditions and media were as similar as possible to cultures used in electrophysiology experiments, except that the mitotic inhibitor 5-fluoro-2-deoxyuridine was added at 4 d in culture to prevent overgrowth of glia.

Viral gene delivery

We used recombinant Semliki Forest virus-based gene delivery to introduce Syt IV into cultured hippocampal neurons. All of our constructs were cloned into the pIRES2–EGFP mammalian expression vector (Clontech, Mountain View, CA) before being shuttled into the Semliki Forest virus plasmid (pSFV; Invitrogen, Carlsbad, CA). Thus, each viral construct contains an internal ribosome entry site (IRES) sequence to allow separate expression of Syts and green fluorescent protein (GFP). The Syt I R233Q point mutant was generated from the Syt I pIRES2–EGFP construct using a Quickchange (Stratagene, La Jolla, CA) strategy with sequence-specific primers to introduce the point mutation and a unique diagnostic restriction site. The point mutation was verified through a restriction digest, and the coding region was subsequently sequenced for verification and subcloned into the pSFV vector. Virions were generated and activated for infection according to the SFV Gene Expression System manual (Invitrogen). Cultured neurons were used for electrophysiological recordings or coimmunoprecipitations at 10–24 h after viral infection.

Biochemistry

At 14–16 d in culture, neurons were harvested with a cell scraper and subjected to 10–15 strokes in a tight-fit dounce homogenizer (Kimble/Kontes, Vineland, NJ) at 4°C in detergent-free buffer. The crude homogenate was centrifuged for 5 min at 1300 × *g* to yield a postnuclear supernatant. Protein concentration was determined by a Bradford protein assay (Bio-Rad, Hercules, CA).

Four Fast Flow nProtein A-Sepharose beads (Amersham Biosciences, Piscataway, NJ) were incubated with monoclonal synaptophysin antibody (Chemicon, Temecula, CA) or monoclonal Syt I antibody (gift from S. Bajjalieh, Department of Pharmacology, University of Washington) overnight at 4°C. The control beads were not incubated with antibody. For each immunoprecipitation reaction, 250–500 μg of postnuclear supernatant was added to 15 μl of packed beads and incubated for 2 h at 4°C. The beads were pelleted and washed three to five times in 1 ml of cold PBS. Proteins were eluted from the pelleted beads with SDS sample buffer, boiled at 100°C for 5 min, and separated by SDS-PAGE on a 10% polyacrylamide gel.

For Western analysis, the separated proteins were transferred to nitrocellulose, and then the filters were blocked at room temperature for 40 min in 5% nonfat dry milk in PBS/0.5% Tween 20 (PBST). The blots were incubated with primary antibody in dilution buffer (PBST/0.1% BSA/1:1000 sodium azide) for 1 h at room temperature or overnight at 4°C. The following primary antibodies were used: Syt IV goat polyclonal (Santa Cruz Biotechnology, Santa Cruz, CA), 1:500, detected a single ~46 kDa band as reported previously (Ferguson et al., 1999); Syt I rabbit polyclonal antibody (gift from S. Bajjalieh), 1:3000, detected an ~65 kDa band specific to Syt I; synaptophysin rabbit polyclonal antibody (Synaptic Systems, Goettingen, Germany), 1:2000, detected an ~38 kDa band; SV2A rabbit polyclonal antibody (gift from S. Bajjalieh), 1:2000, detected an ~95 kDa band; porin mouse monoclonal antibody (Invitrogen), 1:1000, detected an ~33 kDa band. The blots were then washed three times for 15 min in PBST before incubation with HRP-conjugated secondary antibody in 5% milk/PBST. The donkey anti-goat (Jackson ImmunoResearch, West Grove, PA), goat anti-rabbit (Invitrogen), or goat anti-mouse (Invitrogen) HRP-conjugated secondary antibodies were used at 1:2000. The blots were again washed three times for 15 min in PBST before visualization of immunoreactivity by chemiluminescence. The chemiluminescent reaction was performed with SuperSignal Western substrate (Pierce, Rockford, IL), and blot images were acquired with a Kodak (Rochester, NY) Scientific Imaging Station.

Electrophysiology

Whole-cell voltage-clamp recordings of excitatory currents were obtained from isolated autaptic neurons after 10–18 d in microisland culture using a Multiclamp 700A amplifier (Molecular Devices, Sunnyvale, CA). In some experiments, where appropriate, recordings were also obtained from microislands with just a few cells. Such recordings were only included for analysis if the peak of the autaptic EPSC was clearly separated from any polysynaptic currents. All experiments included measurement obtained from two or more different culture preparations and within each preparation were always performed on age-matched neurons that were derived from mice of the same litter.

Recording electrodes of 2–4 MΩ resistance were filled with the following (in mM): 121.5 K-gluconate, 17.5 KCl, 9 NaCl, 1 $MgCl_2$, 10 HEPES, and 0.2 EGTA. To more clearly distinguish excitatory from inhibitory currents, we also performed recordings with a low Cl^- internal solution containing the following (in mM): 157.5 K-gluconate, 1 $MgCl_2$, 10 HEPES, and 0.2 EGTA. The standard extracellular solution consisted of 119 mM NaCl, 5 mM KCl, 2.5 mM $CaCl_2$, 1.5 mM $MgCl_2$, 30 mM glucose, 20 mM HEPES, and 1 μM glycine. The holding current and access resistance were monitored throughout the recordings, and only cells with holding currents <300 pA and stable access resistance were included for analysis. Access resistance was compensated 65–85% to reduce errors in measuring large currents. EPSCs larger than 10 nA (rarely obtained) were completely excluded, because, with such large currents, even a small remaining uncompensated access resistance could result in large measurement errors.

For paired-pulse analysis, the membrane potential was held at −60 mV, and pairs of EPSCs were evoked every 20 s by pairs of stimuli delivered 45 ms apart. The paired-pulse ratio (PPR) was calculated by averaging the peak amplitude of the response to the second pulse over three trials and dividing by the averaged peak amplitude of the response to the first pulse, as recommended by Kim and Alger (2001). We also calculated the PPR at 2.5 mM $[Ca^{2+}]_e$ using the more conventional method of determining the PPR for consecutive pairs of pulses and then averaging the PPR values. These PPR results using this method were identical to the results using the method of Kim and Alger. Spontaneous miniature EPSCs (mEPSCs) were collected and analyzed as reported previously (Sullivan, 1999).

To assess the Ca^{2+} dependence of release, the $[Ca^{2+}]$ of the external recording solution was varied while extracellular magnesium concentration remained constant at 1.5 mM. EPSC peak amplitudes measured in 1, 5, and 10 mM $[Ca^{2+}]_e$ were normalized to the values measured in 2.5 mM $[Ca^{2+}]_e$. The 2.5 mM $[Ca^{2+}]_e$ values were acquired before and after solution changes and then averaged to control for rundown. Solutions were exchanged with a gravity-feed bath perfusion system or by local application from a puffer pipette controlled by a picospritzer with simultaneous rapid clearance through a vacuum pipette. Normalized EPSC values were plotted and fitted to the Dodge–Rahamimoff equation (Dodge and Rahamimoff, 1967), as follows:

$$R(c, m) = \left(\frac{c/K_{Ca}}{1 + \frac{c}{K_{Ca}} + \frac{m}{K_{Mg}}} \right)^k,$$

where $R(c,m)$ is the response size normalized to a maximum value of 1, c is the extracellular calcium concentration, m is the extracellular magnesium concentration, k is a coefficient that determines the degree of co-

operativity and is fixed to a value of 4 (as in the original Dodge–Rahamimoff equation), K_{Ca} is the calcium dissociation constant, and K_{Mg} is the magnesium dissociation constant; concentrations are expressed as millimolar. This equation was fitted to the data using a least squares method in which two parameters were estimated: the calcium dissociation constant and a proportionality constant that described the size of the response. The magnesium dissociation constant was fixed at 8.1 times the value of the calcium dissociation constant (Stevens and Sullivan, 2003). After the fit, all data points were normalized by the proportionality constant so that the maximum response size approached 1. The estimated K_{Ca} is an apparent value, and we do not assume that this estimate reflects the true K_{Ca}; however, this estimate is useful as a tool for assessing alterations in the Ca^{2+}-sensing properties of the Ca^{2+} sensor in neurons.

For the repetitive stimulation protocol, a 20 Hz train of 25 stimuli was delivered every 40 s, and each EPSC in the train was normalized to the peak amplitude of the first EPSC. The repetitive stimulation experiments were performed in standard external recording solution containing 2.5 mM $[Ca^{2+}]_{ext}$. Asynchronous release during a train was quantified as the sum of the asychronous release for each individual response in the train and represents the mean value from at least three consecutive trains for each cell. This value was expressed as a percentage of total release evoked during the train, where total evoked release equals the sum of synchronous and asynchronous release.

For the experiments assessing potential changes in cleft glutamate concentration, we used 0.25 mM γ-D-glutamylglycine (γ-DGG; Tocris Bioscience, Ellisville, MO) and 50 μM cyclothiazide (CTZ; Sigma, St. Louis, MO). Drug applications of 2 min duration were performed by local perfusion from a puffer pipette controlled by a picospritzer with simultaneous rapid clearance through a vacuum pipette. Periods of drug application were always preceded by a stable baseline period and followed by a stable recovery period.

Data analysis. All data were collected using custom software written in Visual Basic 6.0 (Microsoft, Redmond, WA). Data analysis was performed with custom software written in Microsoft C# (courtesy of Ken Custer, University of Washington, Seattle, WA) or Visual Basic 6.0. Curve fitting and K_{Ca} determinations were performed using MathCad 8 (Mathsoft, Cambridge, MA). Plotting of the data was performed using Prism 3.03 (GraphPad, San Diego, CA). Data are reported as mean ± SEM. Values were compared by unpaired Student's *t* test, and *p* values <0.05 are reported as significant.

Detection sensitivity. Small modifications to synaptic release probability (on the order of 5–10% change) may have significant functional impacts if imposed at some critical synapses at the appropriate time. With this in mind, the methods used in this investigation are unlikely to reliably detect changes in fast synaptic transmission of <10%. Therefore, we are unable to completely exclude the possibility that acute Syt IV upregulation produces some very subtle alterations to synaptic transmission in cultured mammalian neurons. However, we feel this is unlikely to be the case based on the following: (1) our experiments were designed to produce a maximal effect by rapidly achieving very strong Syt IV protein upregulation, (2) we used an array of different electrophysiological measures to investigate excitatory neurotransmission, and most importantly, (3) we were able to detect subtle changes in synaptic transmission in our positive control, R233Q-expressing wild-type (WT) neurons.

FM 4-64 imaging

Microisland cultures of hippocampal neurons were mounted in a custom made chamber and bathed in an external solution of 119 mM NaCl, 5 mM KCl, 2.5 mM $CaCl_2$, 1.5 mM $MgCl_2$, 30 mM glucose, 20 mM HEPES, and 1 μM glycine. Dye solutions contained 10 μM FM 4-64 (SynaptoRed C2; Biotium, Richmond, CA). All solutions contained 10 μM CNQX and 50 μM DL-APV to block recurrent activity. Dye solution was superfused over the coverslip, and then vesicle recycling was stimulated by 50 V/cm electrical field stimulation for 1 min at 10 Hz. The dye solution was allowed to remain in the chamber for 1 min after the end of stimulation to ensure optimal loading. The cells were then washed with external solution for 10 min before image acquisition. When selecting fields for imaging, in some cases, microislands with more than one neuron were included, provided that all neurons on these microislands were infected, as indicated by the visual reporter. Once a suitable microisland field was selected, 65 images were acquired at a rate of 1 Hz. Five baseline images were acquired before beginning stimulation. Sixty images were then acquired during 10 Hz electrical stimulation. Image sets were processed by manually selecting the regions of interest (ROIs) of individual puncta using ImageJ (available at http://rsb.info.nih.gov/ij; developed by Wayne Rasband, National Institutes of Health, Bethesda, MD). The integral intensity of each ROI was measured for each image frame and analyzed using Excel (Microsoft) and Prism 3.03 (GraphPad). Destaining rates were determined by curve-fitting to a single exponential decay model. These experiments were conducted using an Olympus (Melville, NY) IX70 inverted microscope with a 40× objective. Sixteen-bit, 512 × 512 images were acquired using MicroMax CCD and WinView software (Princeton Instruments, Trenton, NJ). A mercury arc lamp was used as a UV light source. GFP fluorescence was visualized using a FITC filter set and FM 4-64 fluorescence by using a 515–550 nm excitation and 660 nm long-pass emission filter combination (Chroma Technology, Rockingham, VT). Experiments were performed at room temperature. Data are reported as mean ± SEM. Values were compared by unpaired Student's *t* test, and *p* values <0.05 are reported as significant.

Results

To achieve acute upregulation of Syt IV protein, we infected cultured mouse hippocampal neurons with a viral construct encoding rat Syt IV and GFP. Successfully infected neurons were identified by GFP fluorescence, and strong Syt IV protein elevation in these neurons by 10 h after infection was verified by immunostaining (data not shown). Immunostaining also confirmed that Syt IV expression was below the detection limit in wild-type cultured hippocampal neurons that were not infected with the Syt IV viral construct. Thus, neurons infected with this Syt IV viral construct will subsequently be referred to as Syt IV-expressing neurons.

Upregulated Syt IV protein is trafficked to synaptic vesicles

There are several conflicting reports concerning Syt IV localization on synaptic vesicles (Ferguson et al., 1999; Littleton et al., 1999; Ibata et al., 2002; Adolfsen et al., 2004). To determine whether Syt IV is localized to synaptic vesicles after acute upregulation in our system, we performed a coimmunoprecipitation assay. Cultured neurons were infected (~70% efficiency) with either the Syt IV viral construct or a viral construct encoding GFP alone. Immunoprecipitation of intact synaptic vesicles was performed with either synaptophysin or Syt I monoclonal antibodies. Control immunoprecipitations were performed in the absence of antibody. The immunoprecipitates were then examined by Western blot analysis for the presence of Syt IV, known synaptic vesicle proteins Syt I, SV2A, and synaptophysin, and the mitochondrial membrane protein porin. As expected, immunoreactivity of Syt I, SV2A, and synaptophysin (but not porin) was strongly enriched in the pellet of the synaptophysin and Syt I immunoprecipitations relative to the control immunoprecipitation for both GFP- and Syt IV-expressing neurons (Fig. 1, representative blot). Syt IV immunoreactivity in Syt IV-expressing neurons (detected as a single ~46 kDa band) was also enriched in the pellet of synaptophysin and Syt I immunoprecipitations relative to the control immunoprecipitation, whereas neurons expressing GFP alone had no detectable Syt IV immunoreactivity (Fig. 1). These results were confirmed in three separate coimmunoprecipitation experiments. We note the detection of Syt IV immunoreactivity above background signal in the control immunoprecipitation for Syt IV-expressing neurons; however, this is not unexpected, given the strong elevation of Syt IV protein in these neurons. Together, this evidence indicates that upregulated Syt IV protein is trafficked to synaptic vesicles, including vesicles that also contain Syt I.

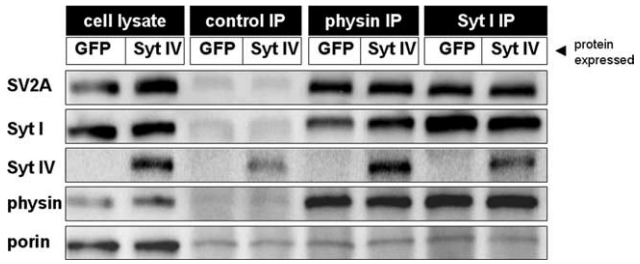

Figure 1. Upregulated Syt IV protein coimmunoprecipitates with synaptic vesicles in cultured neurons. Cultured neurons were infected with either the Syt IV or GFP viral constructs 15 h before harvesting and homogenization. The cleared cell lysate (250–500 μg of protein) was incubated with anti-synaptophysin or anti-synaptotagmin protein A Sepharose beads in the absence of detergent to immunoprecipitate (IP) intact synaptic vesicles (physin IP or Syt I IP, respectively). The control IP was performed with no antibody. Bound proteins were eluted and resolved on an SDS gel and then subjected to immunoblotting with the following antibodies (top to bottom): anti-SV2A, anti-Syt I, anti-Syt IV, anti-synaptophysin, and anti-porin. Cell lysate (1:50 of the IP input) served as a positive control.

Basal release probability is not altered by acute upregulation of Syt IV

To investigate the function of Syt IV upregulation in synaptic transmission, we performed whole-cell voltage-clamp recordings from isolated autaptic hippocampal neurons at 10–18 d in culture. If Syt IV is an inhibitor of neurotransmitter release, then acute upregulation of Syt IV in our neurons is expected to reduce the peak amplitude of EPSCs. We compared EPSC amplitudes of Syt IV-expressing neurons to EPSC amplitudes for uninfected neurons, neurons expressing GFP alone, and neurons overexpressing Syt I and found no significant differences (WT, 3026 ± 362 pA, $n = 30$; GFP, 2947 ± 320 pA, $n = 24$; Syt IV, 2784 ± 471 pA, $n = 25$; Syt I, 2742 ± 401 pA, $n = 11$) (Fig. 2*A*). We also compared the total charge transfer by integrating the area under the EPSCs. As with EPSC peak amplitude, there was no significant difference in mean EPSC charge for Syt IV-expressing neurons relative to control neurons (WT, 22.9 ± 3.3 pC, $n = 30$; GFP, 25.2 ± 2.6 pC, $n = 24$; Syt IV, 23.0 ± 4.5 pC, $n = 25$; Syt I, 23.2 ± 3.9 pC, $n = 11$) (Fig. 2*B*).

As a positive control and demonstration of our detection sensitivity, we infected neurons with a viral construct encoding the Syt I R233Q point mutant (R233Q). Like Syt IV, this mutant exhibits impaired Ca^{2+}-dependent phospholipid binding in the C2A domain (relative to wild-type Syt I), and previous characterization of R233Q knock-in neurons revealed a 50% reduction in EPSC peak amplitude (Fernandez-Chacon et al., 2001). We reasoned that if an overexpressed Syt protein with altered Ca^{2+}-dependent phospholipid binding activity is able to interact with the primary Ca^{2+} sensor to alter release, then expression of R233Q in wild-type neurons should reduce EPSC size. We found that R233Q-expressing neurons had both significantly reduced EPSC peak amplitude (1980 ± 320 pA; $n = 26$) and charge (15.7 ± 2.6 pC; $n = 26$). When compared with neurons expressing GFP alone, the mean EPSC peak amplitude was reduced by 32.8% ± 0.11%, and the mean EPSC charge was reduced by 37.5% ± 0.10% ($p = 0.04$ and 0.01, respectively; unpaired Student's *t* test) (Fig. 2).

We also assessed the peak amplitude of spontaneous mEPSCs and found no significant difference in mean mEPSC size (WT, 19.1 ± 1.1 pA, $n = 16$; GFP, 18.9 ± 1.1 pA, $n = 15$; Syt IV, 17.4 ± 1.0 pA, $n = 15$; Syt I, 18.4 ± 1.1 pA, $n = 10$; R233Q, 18.3 ± 1.4 pA, $n = 10$). The finding that R233Q-expressing neurons have a reduced evoked response size but unaltered mEPSC size is evidence for a reduction in presynaptic basal release probability rather than altered vesicle content or a postsynaptic effect. In contrast, Syt IV upregulation did not alter the size of evoked or spontaneous release events, indicating Syt IV upregulation has no acute effect on basal release probability. In addition, we did not detect any significant difference in mEPSC frequency for Syt IV-expressing neurons relative to WT neurons or neurons expressing GFP alone (WT, 3.3 ± 0.68/s, $n = 25$; WT/GFP, 3.3 ± 1.10/s, $n = 16$; WT/Syt IV, 3.9 ± 1.68/s, $n = 18$; $p = 0.76$, unpaired Student's *t* test for WT/GFP compared with WT/Syt IV), arguing against an alteration to the number of functional synapses with acute Syt IV upregulation.

Ca^{2+} dependence of release is not altered by acute upregulation of Syt IV

Previous reports indicate that Syt IV has diminished Ca^{2+} binding properties relative to Syt I (Ullrich et al., 1994; von Poser et al., 1997). Although upregulation of Syt IV did not alter EPSC peak amplitude or charge, it is still possible that Syt IV upregulation alters the Ca^{2+} dependence of neurotransmitter release. Therefore, we assessed the Ca^{2+} dependence of release by varying the external Ca^{2+} concentration (with Mg^{2+} concentration fixed at 1.5 mM) and measuring the corresponding changes in EPSC peak amplitudes. These data were fitted to the Dodge–Rahamimoff equation to derive Ca^{2+} dependence curves to estimate the apparent Ca^{2+} affinity (K_{Ca}) of the Ca^{2+} sensor for release (Stevens and Sullivan, 2003) (see Materials and Methods). We compared the Ca^{2+} dependence of Syt IV-expressing neurons to the Ca^{2+} dependence for uninfected neurons, neurons expressing GFP alone, and neurons overexpressing Syt I and found that a single Ca^{2+} dependence curve was sufficient to fit all these data. In agreement with this point, the estimated values of K_{Ca} for these groups were nearly indistinguishable (K_{Ca} values in mM: WT, 0.35, $n = 16$; GFP, 0.36, $n = 14$; Syt IV, 0.36, $n = 10$; Syt I, 0.37, $n = 6$) (Fig. 3), indicating that acute upregulation of Syt IV does not alter the Ca^{2+} dependence of release.

One might argue that the failure to detect altered Ca^{2+} dependence of release after Syt IV upregulation was attributable to inadequate sensitivity of the assay. Therefore, to demonstrate the sensitivity of this assay, we measured the Ca^{2+} dependence of release for R233Q-expressing neurons. We detected a 29% increase in the K_{Ca} ($K_{Ca} = 0.45$ mM; $n = 6$) (Fig. 3*B*) for neurons expressing R233Q, which indicates a decrease in the apparent Ca^{2+} affinity of the Ca^{2+} sensor for release. Consistent with this finding, we also detected an even more severe decrease in the apparent Ca^{2+} affinity for Syt I null neurons rescued by expression of R233Q ($K_{Ca} = 0.88$ mM; $n = 2$) (Fig. 3*B*) in which all functional synapses contain only the mutant Syt I protein, and thus the acting Ca^{2+} sensor is formed by R233Q alone (Fernandez-Chacon et al., 2001; Stevens and Sullivan, 2003; Sorensen et al., 2003).

Short-term synaptic plasticity is not altered by acute upregulation of Syt IV

To investigate the effect of Syt IV upregulation on short-term plasticity, we measured the response to pairs of stimuli (PPR) over a range of external Ca^{2+} concentrations. Cultured hippocampal neurons normally exhibit paired-pulse depression (i.e., PPR <1) in standard recording solution (Mennerick and Zorumski, 1995). As expected, in 2.5 mM $[Ca^{2+}]_e$, uninfected neurons and neurons expressing GFP alone showed paired-pulse depression with mean PPR values of 0.82 ± 0.03 ($n = 35$) and 0.78 ± 0.05 ($n = 27$), respectively, and were not significantly different from neurons expressing Syt IV (PPR, 0.82 ± 0.04; $n =$

24) or overexpressing Syt I (PPR, 0.79 ± 0.06; $n = 9$) (Fig. 4*B*). Similarly, no significant differences in the PPR were detected at any of the other $[Ca^{2+}]_e$ tested for these groups (Fig. 4*A*). In contrast, neurons expressing R233Q had a mean PPR of 1.00 ± 0.04 in 2.5 mM $[Ca^{2+}]_e$ ($n = 20$), which was significantly higher than neurons expressing GFP alone ($p < 0.01$; unpaired Student's t test) (Fig. 4*B*). This indicates that R233Q expression reduces paired-pulse depression (increases PPR), consistent with a decrease in basal release probability, whereas Syt IV upregulation has no effect on PPR.

We next investigated whether Syt IV upregulation altered the response to a train of stimuli. We stimulated neurons with a 25 pulse train at 20 Hz once every 40 s and assessed the rate of depression by normalizing the amplitude of each EPSC to the amplitude of the first EPSC in the train. We compared the rate of depression of Syt IV-expressing neurons ($n = 13$) to the rate of depression for uninfected neurons ($n = 16$), neurons expressing GFP alone ($n = 11$), and neurons overexpressing Syt I ($n = 7$). We found the rate of depression indistinguishable between these groups (Fig. 5). In contrast, when we assessed R233Q-expressing neurons ($n = 14$), we detected a slower rate of depression (Fig. 5), which was again consistent with a reduction in basal release probability. In any case, Syt IV-expressing neurons did not exhibit altered PPRs or rate of depression during train stimulation relative to control neurons, indicating that acute upregulation of Syt IV does not alter short-term synaptic plasticity.

In addition, we analyzed our data from the repetitive stimulation experiment to determine whether acute Syt IV upregulation alters the slower asynchronous component of release. We quantified the asynchronous release during the train as a percentage of the total evoked release during the train (where total evoked release equals the sum of synchronous and aysnchronous release) for neurons expressing GFP alone and Syt IV-expressing neurons and found no significant difference (WT/GFP, 47.5% ± 3.4%, $n = 11$; WT/Syt IV, 49.5% ± 3.1%, $n = 13$; unpaired Student's t test, $p = 0.65$). Thus, acute SytIV upregulation does not alter the fraction of total evoked release attributed to asynchronous release, indicating no change in the ratio of synchronous to asynchronous release.

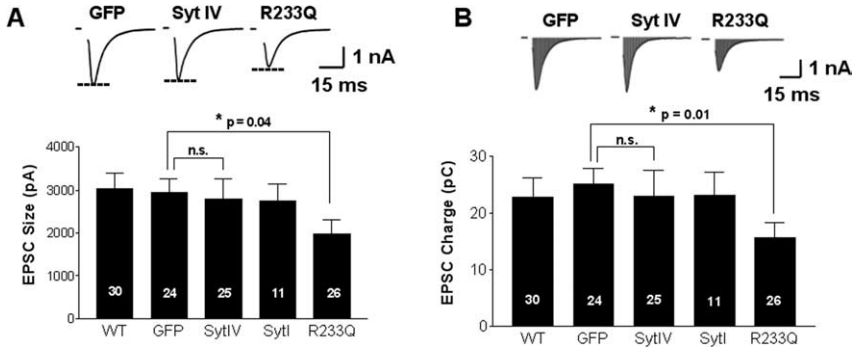

Figure 2. Basal release probability is not altered by acute upregulation of Syt IV. ***A***, Top, Representative EPSCs recorded from cultured autaptic mouse neurons expressing GFP, Syt IV, or R233Q. Delivery of a 1 ms step depolarization to +40 mV initiates an unclamped presynaptic action current (blanked for clarity) followed by an EPSC. The peak amplitude of each EPSC is indicated by a dotted line. Bottom, Summary of average EPSC size for uninfected wild-type neurons and neurons expressing the indicated proteins. The number of neurons in each group is indicated, and plotted values represent the mean ± SEM. *$p = 0.04$ (unpaired Student's t test). ***B***, Top, Representative EPSCs recorded from cultured autaptic mouse neurons expressing GFP, Syt IV, or R233Q. The shaded region is the EPSC charge. Bottom, Summary of average EPSC charge for uninfected wild-type neurons and neurons expressing the indicated proteins. The number of neurons in each group is indicated, and plotted values represent the mean ± SEM. *$p = 0.01$ (unpaired Student's t test). n.s., Not significant.

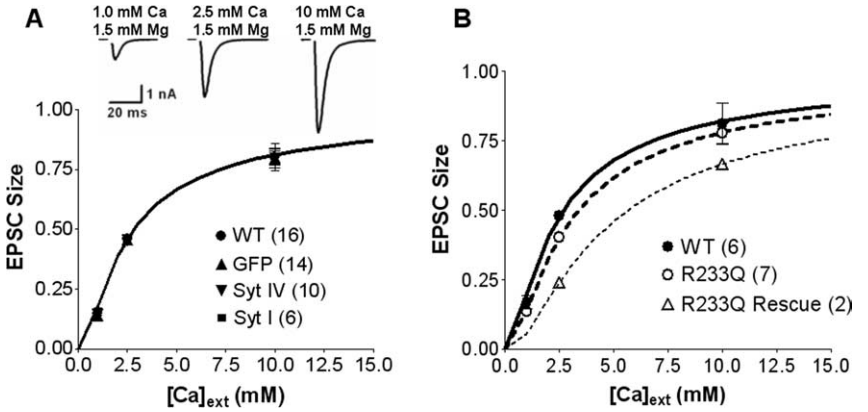

Figure 3. Ca^{2+} dependence of release is not altered by acute upregulation of Syt IV, whereas R233Q-expressing neurons exhibit altered Ca^{2+} dependence of release. ***A***, Top, Representative EPSCs recorded from a wild-type autaptic neuron in 1, 2.5, and 10 mM external calcium. External magnesium concentration was held constant at 1.5 mM. Bottom, Relative EPSC size plotted versus external calcium concentration. (Note: in some cases, the plotted values are nearly indistinguishable.) The solid line is a best fit to the Dodge–Rahamimoff equation that enabled us to obtain an estimate of the K_{Ca} for uninfected wild-type neurons (K_{Ca} = 0.35 mM; see Materials and Methods). Neurons expressing GFP, Syt IV, or Syt I had K_{Ca} values very similar to those for wild-type neurons (K_{Ca} = 0.36, 0.36, and 0.37 mM, respectively) and were well described by the wild-type calcium dependence curve. ***B***, Relative EPSC size plotted versus external calcium concentration for neurons expressing R233Q (open circles). These data were best fit by a calcium dependence curve where K_{Ca} = 0.45 mM (dashed line). Note the rightward shift of the R233Q curve relative to the matched wild-type control curve. A third Ca^{2+}-dependence curve where K_{Ca} = 0.88 mM (dotted line) is shown for R233Q rescue of Syt I null neurons (open triangles). The R233Q rescue curve shows an even stronger rightward shift relative to the wild-type curve. The number of neurons in each group is indicated, and plotted values represent the mean ± SEM. The error bars at some points are smaller than the symbols. $[Ca]_{ext}$, External calcium concentration.

Kinetics of neurotransmitter release are not altered by acute upregulation of Syt IV

Although our findings demonstrate that acute upregulation of Syt IV did not alter the size of evoked or spontaneous release events, these parameters can be distinct from the kinetics of exocytosis. In support of this view, a previous study on PC12 cells reported that Syt IV overexpression altered fusion pore kinetics without altering amperometric spike amplitude or quantal size (Wang et al., 2001). Therefore, we devised experiments to directly test whether Syt IV modulates neurotransmitter release through changes in fusion pore kinetics in cultured mammalian CNS neurons. One line of evidence suggests that Syt IV preferentially promotes the formation of a reversible narrow fusion pore over the formation of an irreversible fusion pore that rapidly and completely dilates (Wang et al., 2003). Release in the former mode is thought to correspond to kiss-and-run exocytosis, whereas release in the latter mode would represent exocytosis via full fusion. Furthermore, it has been proposed that the formation of a reversible narrow fusion pore may lead to subquantal release of gluta-

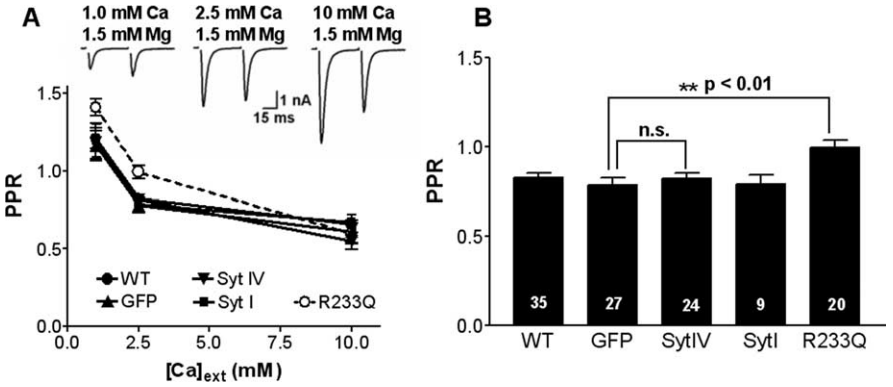

Figure 4. Paired-pulse ratio is not altered by acute upregulation of Syt IV but is increased by expression of Syt I R233Q. ***A***, Top, Representative EPSCs recorded in paired-pulse mode from a wild-type autaptic neuron in 1, 2.5, and 10 mM external calcium ($[Ca]_{ext}$). External magnesium concentration is held constant at 1.5 mM. The membrane potential was clamped at −60 mV, and EPSCs were evoked by a pair of 1 ms depolarizing steps delivered 45 ms apart. The paired-pulse ratio is defined as the peak amplitude of the second EPSC relative to the first EPSC. Bottom, PPR plotted versus external calcium concentration. ***B***, Bar graph of PPRs in 2.5 mM external calcium. The number of neurons in each group is indicated, and plotted values represent the mean ± SEM. $^{**}p < 0.01$ (unpaired Student's *t* test). n.s., Not significant.

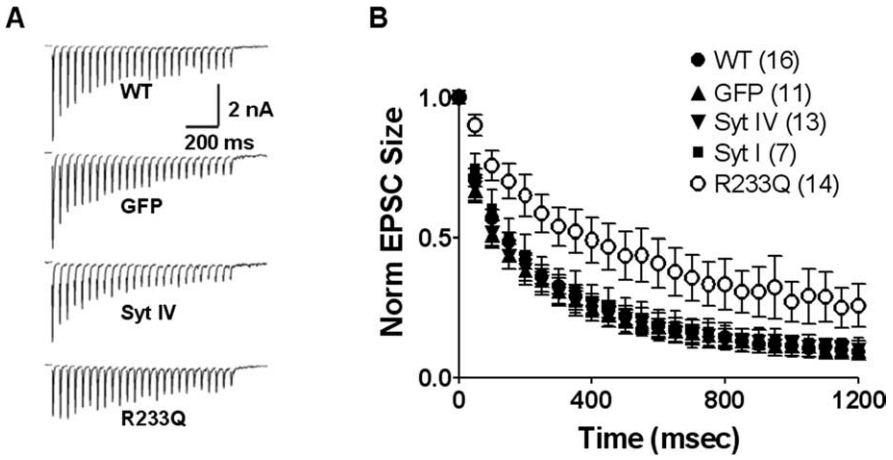

Figure 5. Rate of depression during 20 Hz stimulation is not altered by acute upregulation of Syt IV but is reduced by expression of Syt I R233Q. ***A***, Example EPSCs in response to a stimulus train of 25 pulses at 20 Hz. Data were collected at a rate of one train every 40 s to allow full recovery between stimuli. ***B***, The peak amplitude of each EPSC in the train was normalized (Norm) to the peak amplitude of the first EPSC and plotted versus time to show the rate of depression. The number of neurons in each group is indicated, and plotted values represent the mean ± SEM.

mate (for review, see Rahamimoff and Fernandez, 1997), in which case Syt IV upregulation would be expected to reduce peak glutamate concentration in the synaptic cleft during evoked release. To test this hypothesis, we assessed the degree to which EPSCs were blocked by application of the low-affinity glutamate antagonist γ-DGG. The degree of block served as a measure of the relative peak glutamate concentration in the synaptic cleft. If Syt IV causes a reduction in peak cleft glutamate concentration at individual synapses, then the degree of EPSC block should be increased in Syt IV-expressing neurons relative to control. However, we found that 0.25 mM γ-DGG application produced nearly identical block of EPSC peak amplitude for all groups (percentage block: WT, 48.6 ± 2.8, $n = 14$; GFP, 48.5 ± 2.8, $n = 14$; Syt IV, 49.3 ± 3.3, $n = 12$; Syt I, 49.8 ± 2.2, $n = 10$) (Fig. 6*A*). The same result was obtained for the analysis of EPSC charge in this experiment (data not shown). We also noted that γ-DGG application did not alter the PPR for any of the groups investigated, indicating a similar degree of block on both the first and second pulse (data not shown), a result inconsistent with altered fusion pore kinetics as a mechanism underlying short-term depression at these synapses.

An alternative hypothesis is that Syt IV modulates the fusion pore to prevent a rapid spike in glutamate concentration in the cleft. In this scenario, glutamate flux from the vesicle lumen into the synaptic cleft would proceed through a narrow fusion pore that is stabilized for a prolonged duration, thereby allowing the gradual release of the full complement of glutamate of a vesicle into the cleft. Effectively, there would not be a rapid spike of glutamate concentration in the cleft, and the prolonged presence of a low concentration of glutamate would lead to AMPA receptor desensitization (Choi et al., 2000; Klyachko and Jackson, 2002; Wang et al., 2003). This hypothesis predicts that a postsynaptic response would be profoundly diminished and perhaps undetectable, because the peak cleft glutamate concentration does not reach a level sufficient for activating significant numbers of AMPA receptors before the onset of receptor desensitization. To test this hypothesis, we measured EPSC amplitudes in the presence of the AMPA receptor-desensitization blocker cyclothiazide. If Syt IV leads to receptor desensitization by causing a slow release of glutamate for a prolonged duration, then application of CTZ would reveal a component of glutamate release that was not detectable before drug application [for modeling of the CTZ effect, see also Choi et al. (2003)]. However, we found that the enhancement of EPSC size in the presence of CTZ was not significantly different for Syt IV-expressing neurons relative to uninfected neurons or neurons expressing GFP alone (CTZ enhancement, normalized to predrug EPSC amplitude: WT, 1.59 ± 0.11, $n = 7$; GFP, 1.48 ± 0.18, $n = 5$; Syt IV, 1.42 ± 0.07, $n = 7$) (Fig. 6*B*). We noted that CTZ application had an even more profound effect on EPSC charge than EPSC peak amplitude, but as with the peak amplitude, we did not detect an increased enhancement of EPSC charge during CTZ application to Syt IV-expressing neurons (CTZ enhancement, normalized to predrug EPSC charge: WT, 3.89 ± 0.60, $n = 7$; GFP, 4.33 ± 0.74, $n = 5$; Syt IV, 3.34 ± 0.40, $n = 7$).

Mode of neurotransmitter release is not altered by acute upregulation of Syt IV

Changes in the mode of exocytosis (full fusion vs kiss-and-run) have been detected in the absence of altered electrophysiological measures of neurotransmitter release (Stevens and Williams, 2000). Thus, in addition to electrophysiological techniques, we used optical measurements of exocytosis to investigate the possible modulation of the fusion pore by acute upregulation of Syt IV. Promotion of kiss-and-run fusion reduces the amount of the styryl dye FM 1-43 released from dye-loaded vesicles in cultured hippocampal neurons (Stevens and Williams, 2000; Aravanis et

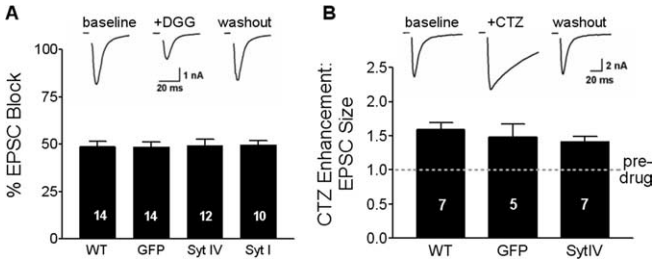

Figure 6. Kinetics of neurotransmitter release are not altered by acute upregulation of Syt IV. ***A***, Degree of EPSC block (percentage) during application of 0.25 μM γ-DGG. The degree of block is measured as the reduction in EPSC peak amplitude relative to the average of predrug and washout EPSC peak amplitude. Inset, Example EPSC traces of predrug baseline, γ-DGG application, and EPSC recovery after drug washout for an uninfected wild-type neuron. ***B***, EPSC peak amplitudes measured during application of 50 μM CTZ and normalized to predrug EPSC size (dotted line). Inset, Example EPSC traces of predrug baseline, CTZ application, and EPSC recovery after drug washout for a Syt IV-expressing neuron. The number of neurons in each group is indicated, and plotted values represent the mean ± SEM.

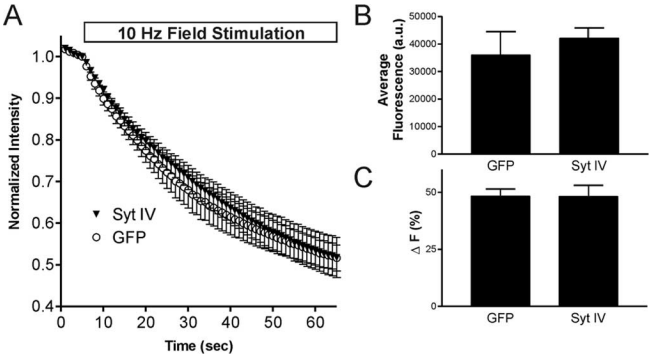

Figure 7. Rate of FM 4-64 destaining is not altered by acute upregulation of Syt IV. ***A***, Time course of FM 4-64 fluorescence changes during electrical field stimulation at 10 Hz for 1 min. At each time point, the fluorescence of the release sites was normalized to the fluorescence value obtained immediately preceding stimulation. Images were collected at a rate of 1 Hz. ***B***, Average fluorescence values of release sites obtained from the first image acquired during destaining experiments. ***C***, Average percentage of the total fluorescence lost during the 10 Hz stimulation period. Values were calculated from five GFP and five Syt IV experiments with 20 release sites from each experiment, for a total of 100 release sites analyzed per group. Plotted values represent the mean ± SEM. a.u., Arbitrary units.

al., 2003; Richards et al., 2005). If upregulation of Syt IV promotes kiss-and-run in neurons, as it does in PC12 cells (Wang et al., 2003), we would predict a reduction in the rate and total amount of dye release from loaded synapses during trains of action potentials in Syt IV-expressing neurons. To test this, we used the red variant dye FM 4-64 to load recycling pools of vesicles in Syt IV-expressing neurons or neurons expressing GFP alone and studied the kinetics of dye release by monitoring changes in fluorescence during 1 min of 10 Hz electrical field stimulation (Fig. 7). We observed no significant difference in the rate of destaining during 10 Hz stimulation between the two groups ($t_{(1/2)} = 26.5 \pm 7.4$ and 28.2 ± 3.4 s for GFP and Syt IV, respectively; $n = 5$ microisland fields, 20 release sites per field, 100 total release sites analyzed per group). In addition, we detected no significant difference between the two groups in the initial absolute fluorescence intensity of loaded puncta (i.e., dye loaded) or in the fraction of initial fluorescence of each puncta lost after stimulation (i.e., dye lost). These results demonstrate that acute upregulation of Syt IV does not alter fusion pore properties in a way that would affect FM dye loss and thus indicate that Syt IV does not promote kiss-and-run exocytosis in mammalian CNS neurons.

Discussion

The most distinct properties of the Syt IV protein are reduced Ca^{2+} binding in the C2A domain because of a naturally occurring amino acid substitution and strong induction in the hippocampus after seizure. We have tested the dominant hypothesis of Syt IV function, which states that Syt IV upregulation after seizure is a neuroprotective mechanism to inhibit neurotransmitter release. We sought to determine whether Syt IV functions by negatively regulating the Ca^{2+} sensor for exocytosis in mammalian CNS neurons. We overexpressed Syt IV protein in cultured mouse hippocampal neurons and used biochemical, electrophysiological, and optical techniques to assess protein localization and acute effects on excitatory neurotransmission. Although upregulated Syt IV protein is trafficked to synaptic vesicles, we found fast neurotransmission unaltered with respect to basal release probability, Ca^{2+} dependence of release, short-term plasticity, and fusion pore kinetics. Furthermore, acute Syt IV upregulation did not alter the size or frequency of spontaneous release events or the ratio of synchronous to asychronous release. In contrast, expression of Syt I R233Q reduced release probability and altered the Ca^{2+} dependence of release, thus demonstrating the sensitivity of the system to changes in neurotransmission resulting from changes to the Ca^{2+} sensor. Together, these data are not consistent with the notion Syt IV functions as an acute negative regulator of excitatory neurotransmission.

Our demonstration that upregulated Syt IV protein coimmunoprecipitates with synaptic vesicles supports previous reports that Syt IV is a synaptic vesicle protein (Ferguson et al., 1999; Littleton et al., 1999). Other evidence suggests Syt IV is not sorted predominantly to mature synaptic vesicles (Ibata et al., 2002; Adolfsen et al., 2004); therefore, the specific method and duration of protein induction, as well as the assays and model systems used, may be critical factors in Syt IV trafficking. We conclude that a significant fraction of upregulated Syt IV protein is sorted to synaptic vesicles in our system, and thus, it exhibits the expected localization of a protein involved in presynaptic modulation of neurotransmission.

Our finding that acute Syt IV upregulation did not alter basal release probability is inconsistent with the finding that Syt IV overexpression at the *Drosophila* neuromuscular junction reduced evoked response amplitude (Littleton et al., 1999). However, a more recent study could not replicate this result, despite working with the same preparation (Robinson et al., 2002). The second study investigated overexpression of Syt IV and found no evidence of an inhibitory effect on response amplitude, miniature size, or miniature frequency over a range of $[Ca^{2+}]_e$, which is in accordance with our results. In the study of PC12 cell dense-core vesicle exocytosis, two investigations produced evidence that Syt IV overexpression reduces Ca^{2+}-stimulated release (Wang et al., 2001; Machado et al., 2004). Given the differences between chromaffin cells and neurons (e.g., rate of transmitter release, type of vesicles present, and Syt isoform expression levels and/or ratios), it is possible that the mechanisms controlling neurotransmission are not entirely conserved in these two systems.

The only previously available functional evidence concerning Syt IV in mammalian neurons comes from characterization of Syt IV null mice (Ferguson et al., 2000, 2004). Extracellular field recordings from hippocampal slices revealed that the basal release probability at Schaffer collateral synapses was normal in the absence of Syt IV (Ferguson et al., 2004). Although this finding is

consistent with our data, other electrophysiological evidence from the same study is not. Syt IV null neurons in the CA1 pyramidal field exhibited altered short-term plasticity in the form of enhanced paired-pulse facilitation and post-tetanic potentiation. The authors concluded that Syt IV functions as a negative regulator of short-term synaptic plasticity (Ferguson et al., 2004). In contrast, our whole-cell recordings of hippocampal neurons overexpressing Syt IV protein did not reveal any effect on short-term plasticity. We did not detect any effect on the PPR at several different $[Ca^{2+}]_e$, nor did we detect a difference in the rate of synaptic depression during repetitive stimulation. Perhaps the effects described in the previously published work result from persistent absence of the Syt IV protein, whereas in our investigation, Syt IV upregulation was achieved acutely, as is the case after seizure.

Syt I overexpression did not alter neurotransmission in any of our experiments, which is consistent with findings presented by Virmani et al. (2003). In contrast, a previous report that measured vesicular release probability and used a very similar repetitive stimulation protocol showed that Syt I overexpression in wild-type mouse neurons, also using Semliki Forest virus, increased the probability of release (Han et al., 2004). The authors proposed that Syt I copy number on synaptic vesicles could serve as a key determinant of synaptic release probability. However, this same effect was not apparent when strong Syt I expression was used to rescue transmission in Syt I null neurons (J. T. Ting, unpublished observations) (Stevens and Sullivan, 2003; Han et al., 2004), a scenario in which viral expression is believed to produce Syt I expression well above endogenous levels. More quantitative methods for measuring the number of Syt I molecules on synaptic vesicles are necessary to resolve this issue. With respect to the present investigation, the lack of an effect of Syt I overexpression on release probability suggests that the effect of Syt overexpression on neurotransmission is determined primarily by the properties of the Syt protein expressed and not by copy number of the Syt protein expressed.

Recently, evidence supporting a role for Syt IV in modulating dense-core vesicle fusion pore kinetics in PC12 cells has gained considerable attention. The modulation of neurotransmitter release at a postfusion stage through the regulation of fusion pore diameter and/or open duration could serve as a key mechanism for synaptic plasticity. We addressed three prominent aspects of fusion pore modulation by Syt IV. We first addressed the prediction that Syt IV elevation leads to subquantal glutamate release by promoting exocytosis through a reversible, narrow fusion pore that restricts glutamate release (Wang et al., 2003). Our use of the competitive glutamate antagonist γ-DGG to show that acute Syt IV upregulation does not alter the peak glutamate concentration in the synaptic cleft argues against this hypothesis at mammalian CNS synapses. This view is further supported by the lack of an effect of Syt IV upregulation on EPSC amplitude, EPSC charge, and quantal size. We also investigated the hypothesis that Syt IV promotes formation of a narrow fusion pore that is open for a prolonged duration and thus leads to slow release of the complement of glutamate of a full vesicle (Klyachko and Jackson, 2002; Wang et al., 2003). This hypothesis predicts a component of the postsynaptic response would be lost because the peak cleft glutamate concentration would not reach a level sufficient for activating AMPA receptors before onset of receptor desensitization (Choi et al., 2000; Klyachko and Jackson, 2002; Wang et al., 2003) [for modeling of glutamate release through rapidly expanding and nonexpanding fusion pores, see also Choi et al. (2003) and Pawlu et al. (2004)]. Because we saw no effect of Syt IV on EPSC peak amplitude enhancement when pharmacologically blocking AMPA receptor desensitization, we conclude Syt IV does not alter the time course of glutamate release into the synaptic cleft in the mammalian CNS.

Our finding that neither peak concentration nor time course of glutamate release into the synaptic cleft is altered by acute upregulation of Syt IV is inconsistent with the report that Syt IV elevation promotes kiss-and-run exocytosis over full fusion in PC12 cells (Wang et al., 2003). If, however, kiss-and-run exocytosis does not lead to a reduction in the amount of glutamate release (Stevens and Williams, 2000), then our electrophysiological findings per se are not sufficient to eliminate the possibility that Syt IV elevation promotes kiss-and-run. Thus, we incorporated optical imaging experiments to provide direct evidence that acute Syt IV upregulation does not promote a switch from full fusion to kiss-and-run in mammalian CNS neurons. These findings emphasize that the regulation of neurotransmission may not be entirely conserved between PC12 cells and mammalian CNS neurons.

What function is Syt IV serving in mammalian neurons? One possibility is that the main role of Syt IV is promoting Ca^{2+}-dependent glutamate release from astrocytes, as demonstrated by Zhang et al. (2004). It will be interesting to see whether this phenomenon plays a role in the regulation of neurotransmission. It should be noted that a role for Syt IV in astrocytes would not preclude an additional role in neurons. It remains to be seen whether Syt IV modulates inhibitory neurotransmission, a question beyond the scope of this investigation. Finally, although the available evidence suggests Syt IV protein turnover is rapid (Vician et al., 1995; Tocco et al., 1996), which led us to investigate acute effects on neurotransmission, it is conceivable that Syt IV upregulation leads to some form of long-term modification of synaptic transmission. Although these and other ideas await more detailed investigation, we conclude from this investigation that Syt IV is not an acute negative regulator of fast excitatory neurotransmission and does not promote kiss-and-run exocytosis in mammalian CNS neurons.

References

Adolfsen B, Saraswati S, Yoshihara M, Littleton JT (2004) Synaptotagmins are trafficked to distinct subcellular domains including the postsynaptic compartment. J Cell Biol 166:249–260.

Aravanis AM, Pyle JL, Tsien RW (2003) Single synaptic vesicles fusing transiently and successively without loss of identity. Nature 423:643–647.

Bekkers JM, Stevens CF (1991) Excitatory and inhibitory autaptic currents in isolated hippocampal neurons maintained in cell culture. Proc Natl Acad Sci USA 88:7834–7838.

Choi S, Klingauf J, Tsien RW (2000) Postfusional regulation of cleft glutamate concentration during LTP at 'silent synapses.' Nat Neurosci 3:330–336.

Choi S, Klingauf J, Tsien RW (2003) Fusion pore modulation as a presynaptic mechanism contributing to expression of long-term potentiation. Philos Trans R Soc Lond B Biol Sci 358:695–705.

Dodge Jr FA, Rahamimoff R (1967) Co-operative action of calcium ions in transmitter release at the neuromuscular junction. J Physiol (Lond) 193:419–432.

Ferguson GD, Thomas DM, Elferink LA, Herschman HR (1999) Synthesis, degradation, and subcellular localization of synaptotagmin IV, a neuronal immediate early gene product. J Neurochem 72:1821–1831.

Ferguson GD, Anagnostaras SG, Silva AJ, Herschman HR (2000) Deficits in memory and motor performance in synaptotagmin IV mutant mice. Proc Natl Acad Sci USA 97:5598–5603.

Ferguson GD, Wang H, Herschman HR, Storm DR (2004) Altered hippocampal short-term plasticity and associative memory in synaptotagmin IV (−/−) mice. Hippocampus 14:964–974.

Fernandez-Chacon R, Konigstorfer A, Gerber SH, Garcia J, Matos MF,

Stevens CF, Brose N, Rizo J, Rosenmund C, Sudhof TC (2001) Synaptotagmin I functions as a calcium regulator of release probability. Nature 410:41–49.

Han W, Rhee JS, Maximov A, Lao Y, Mashimo T, Rosenmund C, Sudhof TC (2004) N-glycosylation is essential for vesicular targeting of synaptotagmin 1. Neuron 41:85–99.

Ibata K, Hashikawa T, Tsuboi T, Terakawa S, Liang F, Mizutani A, Fukuda M, Mikoshiba K (2002) Non-polarized distribution of synaptotagmin IV in neurons: evidence that synaptotagmin IV is not a synaptic vesicle protein. Neurosci Res 43:401–406.

Kim J, Alger BE (2001) Random response fluctuations lead to spurious paired-pulse facilitation. J Neurosci 21:9608–9618.

Klyachko VA, Jackson MB (2002) Capacitance steps and fusion pores of small and large-dense-core vesicles in nerve terminals. Nature 418:89–92.

Littleton JT, Serano TL, Rubin GM, Ganetzky B, Chapman ER (1999) Synaptic function modulated by changes in the ratio of synaptotagmin I and IV. Nature 400:757–760.

Machado HB, Liu W, Vician LJ, Herschman HR (2004) Synaptotagmin IV overexpression inhibits depolarization-induced exocytosis in PC12 cells. J Neurosci Res 76:334–341.

Mennerick S, Zorumski CF (1995) Paired-pulse modulation of fast excitatory synaptic currents in microcultures of rat hippocampal neurons. J Physiol (Lond) 488:85–101.

Pawlu C, DiAntonio A, Heckmann M (2004) Postfusional control of quantal current shape. Neuron 42:607–618.

Rahamimoff R, Fernandez JM (1997) Pre- and postfusion regulation of transmitter release. Neuron 18:17–27.

Richards DA, Bai J, Chapman ER (2005) Two modes of exocytosis at hippocampal synapses revealed by rate of FM1-43 efflux from individual vesicles. J Cell Biol 168:929–939.

Robinson IM, Ranjan R, Schwarz TL (2002) Synaptotagmins I and IV promote transmitter release independently of Ca(2+) binding in the C(2)A domain. Nature 418:336–340.

Sorensen JB, Fernandez-Chacon R, Sudhof TC, Neher E (2003) Examining synaptotagmin 1 function in dense core vesicle exocytosis under direct control of Ca^{2+}. J Gen Physiol 122:265–276.

Stevens CF, Sullivan JM (2003) The synaptotagmin C2A domain is part of the calcium sensor controlling fast synaptic transmission. Neuron 39:299–308.

Stevens CF, Williams JH (2000) "Kiss and run" exocytosis at hippocampal synapses. Proc Natl Acad Sci USA 97:12828–12833.

Sullivan JM (1999) Mechanisms of cannabinoid-receptor-mediated inhibition of synaptic transmission in cultured hippocampal pyramidal neurons. J Neurophysiol 82:1286–1294.

Tocco G, Bi X, Vician L, Lim IK, Herschman H, Baudry M (1996) Two synaptotagmin genes, Syt1 and Syt4, are differentially regulated in adult brain and during postnatal development following kainic acid-induced seizures. Brain Res Mol Brain Res 40:229–239.

Ullrich B, Li C, Zhang JZ, McMahon H, Anderson RG, Geppert M, Sudhof TC (1994) Functional properties of multiple synaptotagmins in brain. Neuron 13:1281–1291.

Vician L, Lim IK, Ferguson G, Tocco G, Baudry M, Herschman HR (1995) Synaptotagmin IV is an immediate early gene induced by depolarization in PC12 cells and in brain. Proc Natl Acad Sci USA 92:2164–2168.

Virmani T, Han W, Liu X, Sudhof TC, Kavalali ET (2003) Synaptotagmin 7 splice variants differentially regulate synaptic vesicle recycling. EMBO J 22:5347–5357.

von Poser C, Ichtchenko K, Shao X, Rizo J, Sudhof TC (1997) The evolutionary pressure to inactivate. A subclass of synaptotagmins with an amino acid substitution that abolishes Ca^{2+} binding. J Biol Chem 272:14314–14319.

Wang CT, Grishanin R, Earles CA, Chang PY, Martin TF, Chapman ER, Jackson MB (2001) Synaptotagmin modulation of fusion pore kinetics in regulated exocytosis of dense-core vesicles. Science 294:1111–1115.

Wang CT, Lu JC, Bai J, Chang PY, Martin TF, Chapman ER, Jackson MB (2003) Different domains of synaptotagmin control the choice between kiss-and-run and full fusion. Nature 424:943–947.

Zhang Q, Fukuda M, Van Bockstaele E, Pascual O, Haydon PG (2004) Synaptotagmin IV regulates glial glutamate release. Proc Natl Acad Sci USA